[7]Moroz, B. I., Kerganovich, V. V., and Krasnopolskiy, V. A., "Martian Atmosphere Model for MARS-94 Project (MA-90)," *Space Researches*, Vol. 29, No. 1, 1991, pp. 3–84.

[8]Tauber, M. E., Bowles, J. V., and Yang, L., "The Heating Environment During Martian Atmospheric Descent," *Journal of Spacecraft and Rockets*, Vol. 26, No. 5, 1989, pp. 330–337.

[9]Nelder, I., and Mead, R., "A Simplex Method for Function Minimization," *Computer Journal*, Vol. 7, 1965, pp. 308–313.

T. C. Lin
Associate Editor

Unity Check Method for Structural Damage Detection

Cheng S. Lin*
The Aerospace Corporation,
El Segundo, California 90245-4691

Introduction

IN anticipation of the deployment of large structures in space, researchers have been trying to develop methods to detect and to locate structural damage if it occurs. One promising approach is to use modal data collected from an on-orbit mode survey test to detect critical damage. Damage in the structure causes degradation in its stiffness properties, which in turn changes its mode shapes and frequencies. Assuming that a finite element model has been developed and verified by an earlier mode survey test before damage occurs, the problem of using measured modes and frequencies from a later mode survey test to detect damage is equivalent to trying to correct a defective finite element model using mode survey test data.

Several researchers have developed different methods to locate the physical positions of modeling errors.[1–4] The author has proposed a unity check method to locate modeling errors in stiffness using modal test data.[5] This Note applies the method to locate structural damage and, furthermore, to determine the magnitudes of stiffness reduction in the damaged elements by the least-squares technique. It is assumed that the analytical model of the original structure has been satisfactorily verified by a mode survey test.

Theoretical Formulation

It can be proved that the following relationships are true for an n-degree-of-freedom linear dynamic system[5]:

$$[K] = [M]\left(\sum_{i=1}^{n} \omega_i^2\{\phi_i\}\{\phi_i\}^T\right)[M] \tag{1}$$

$$[f] = [\phi][\omega^{-2}][\phi]^T = \sum_{i=1}^{n} \omega_i^{-2}\{\phi_i\}\{\phi_i\}^T \tag{2}$$

where $[K]$, $[f]$, and $[M]$ are the stiffness, flexibility, and mass matrices, respectively; ω_i is the ith modal frequency; $\{\phi_i\}$ is the ith modal vector; $[\phi]$ is the modal matrix; and $[\omega]$ is the modal frequency matrix. From Eq. (1), it can be seen that modal contribution to the stiffness matrix increases as the modal frequency increases, whereas Eq. (2) reveals that the flexibility matrix converges rapidly as the frequency increases.

In the mode survey test for the potentially damaged structure, only the lowest few modes can be accurately measured because of instrument limitation. Therefore, the flexibility matrix for the damaged structure can be best approximated by the following partitioned expression:

$$[f_d] = [\phi_{ld} \quad \phi_{hu}]\begin{bmatrix}\omega_{ld}^{-2} & \\ & \omega_{hu}^{-2}\end{bmatrix}[\phi_{ld} \quad \phi_{hu}]^T \tag{3}$$

where subscripts d and u denote the damaged and undamaged structure, respectively; subscripts l and h indicate the lower and higher modes, respectively. The stiffness matrix for the damaged structure is

$$[K_d] = [K_u] - [\Delta K] \tag{4}$$

where $[\Delta K]$ is the changes in stiffness due to the damage. By definition,

$$[f_d][K_d] = [I] \tag{5}$$

Substituting Eq. (4) into Eq. (5), one obtains the following:

$$[f_d][\Delta K] = [E] \tag{6}$$

where

$$[E] = [f_d][K_u] - [I] \tag{7}$$

Because $[\Delta K]$ results from the damage, it will have nonzero values only at degrees of freedom connected to the damaged members. Therefore, Eq. (6) can be partitioned as follows:

$$[\bar{f}_{da} \quad \bar{f}_{db}]\begin{bmatrix}0 & 0\\ 0 & \Delta\bar{K}\end{bmatrix} = [\bar{E}_a \quad \bar{E}_b] \tag{8}$$

where $\Delta\bar{K}$ is the nonzero submatrix of $[\Delta K]$, $\bar{f}_{da}$ and $\bar{f}_{db}$ are submatrices of $[f_d]$, and $\bar{E}_a$ and $\bar{E}_b$ are submatrices of $[E]$. It can be seen that $\bar{E}_b$ will have significant values and $\bar{E}_a$ will not. Furthermore, the error of each degree of freedom can be measured by the maximum absolute value of elements in the corresponding column of $[E]$, namely,

$$\varepsilon_j = \max_{i=1}^{n} |e_{ij}| \tag{9}$$

By inspecting the magnitudes of ε_j, one can identify the affected degrees of freedom.

Dropping the subscript b in $\bar{f}_{db}$ and $\bar{E}_b$ for simplicity, Eq. (8) can be simplified as follows:

$$\underset{n\times l}{[\bar{f}_d]}\ \underset{l\times l}{[\Delta\bar{K}]} = \underset{n\times l}{[\bar{E}]} \tag{10}$$

where l is the total number of affected degrees of freedom. Because $[\bar{f}_d]$ and $[\bar{E}]$ are known, Eq. (10) represents a set of linear constraints for the elements of $[\Delta\bar{K}]$. To facilitate the solution for $[\Delta\bar{K}]$, Eq. (10) is transformed into the standard form for a system of overdetermined simultaneous equations as follows:

$$\underset{nl\times ll}{[\tilde{f}_d]}\ \underset{ll\times l}{\{\Delta\hat{K}\}} = \underset{nl\times l}{\{\hat{E}\}} \tag{11}$$

where

$$[\tilde{f}_d] = \begin{bmatrix}\bar{f}_d & 0 & \cdots & 0\\ 0 & \bar{f}_d & \cdots & 0\\ \vdots & \vdots & \ddots & \vdots\\ 0 & 0 & \cdots & \bar{f}_d\end{bmatrix} \tag{12}$$

and where $\{\Delta\hat{K}\}$ and $\{\hat{E}\}$ are column vectors formed by stacking columns of $[\Delta\bar{K}]$ and $[\bar{E}]$, respectively. Furthermore, from the affected degrees of freedom and their connectivity, one can identify the structural members that may have been damaged. Such identification does not have to be exclusive. In the succeeding numerical

Received Aug. 5, 1997; revision received March 30, 1998; accepted for publication April 6, 1998.

*Engineering Specialist, Structural Dynamics Department, 2350 E. El Segundo Boulevard. Senior Member AIAA.

example, it will be demonstrated that the proposed method works even if undamaged members are included in the suspect list. The $[\Delta\bar{K}]$ can be expressed as the summation of stiffness changes of all potentially damaged members, namely,

$$[\Delta\bar{K}] = \sum_{i=1}^{m} \delta_i [k_i] \tag{13}$$

where δ_i is the reduction coefficient and $[k_i]$ is the $l \times l$ element stiffness matrix of ith potentially damaged member, or, in the vector form,

$$\{\Delta\hat{K}\} = \sum_{i=1}^{m} \delta_i \{\hat{k}_i\} = [\hat{k}_1 \quad \hat{k}_2 \quad \cdots \quad \hat{k}_m] \begin{Bmatrix} \delta_1 \\ \delta_2 \\ \vdots \\ \delta_m \end{Bmatrix} \tag{14}$$

where $\{\Delta\hat{K}\}$ and $\{\hat{k}_i\}$ are vectorized $[\Delta\bar{K}]$ and $[k_i]$, respectively, by stacking columns together; and m is the total number of potentially damaged members. Substituting Eq. (14) into Eq. (11), one obtains

$$\underset{nl \times m}{[H]} \; \underset{m \times l}{\{\delta\}} = \underset{nl \times l}{\{\hat{E}\}} \tag{15}$$

where

$$[H] = [\tilde{f}_d][\hat{k}_1 \quad \hat{k}_2 \quad \cdots \quad \hat{k}_m] \tag{16}$$

$$\{\delta\} = \begin{Bmatrix} \delta_1 \\ \delta_2 \\ \vdots \\ \delta_m \end{Bmatrix} \tag{17}$$

A least-squares solution to Eq. (15) can then be obtained as follows:

$$\{\delta\} = ([H]^T[H])^{-1}[H]^T\{\hat{E}\} \tag{18}$$

The solution involves inversion of an $m \times m$ matrix. The $\{\delta\}$ will reveal the fractional reduction of stiffness in each identified damaged member.

Numerical Example

The proposed method will be applied to a cantilevered planar six-bay truss with two translational degrees of freedom at each node. The geometry and material properties of the undamaged structure are shown in Fig. 1a, and the stiffness is assumed to have been verified by a mode survey test. Damage to the structure is simulated by reducing Young's moduli of the damaged members. Shown in Fig. 1b is the damaged structure of which members f, g, and h are damaged. Measured modes of the damaged structure are simulated by its analytically calculated modes. These modes are supplemented by the analytical modes of the undamaged structure to determine the flexibility matrix of the damaged structure. The calculated natural frequencies of the undamaged and damaged structures are compared in Table 1.

The unity check errors for the damaged structure using four and eight measured modes are shown in Table 2. Significant errors occur only at degrees of freedom connected to the damaged members. Based on the connectivity, five members are identified as suspects for having been damaged and are included in the solution for stiffness reductions. The resulting stiffness reductions are shown in Table 3. The two undamaged members are found to suffer negligible stiffness reduction, and the reductions in the three damaged members are accurately determined.

Discussion

In the foregoing numerical example, the proposed method requires few modes to obtain accurate results, indicating that the damaged members have been sufficiently exercised by the first few

Table 1 Comparison of natural frequencies for undamaged and damaged structures

Mode no.	Undamaged, Hz	Damaged, Hz
1	2.59	2.53
2	13.78	13.07
3	26.25	24.70
4	32.25	30.46
5	51.69	48.61
6	68.96	64.79
7	76.54	72.23
8	81.07	76.69

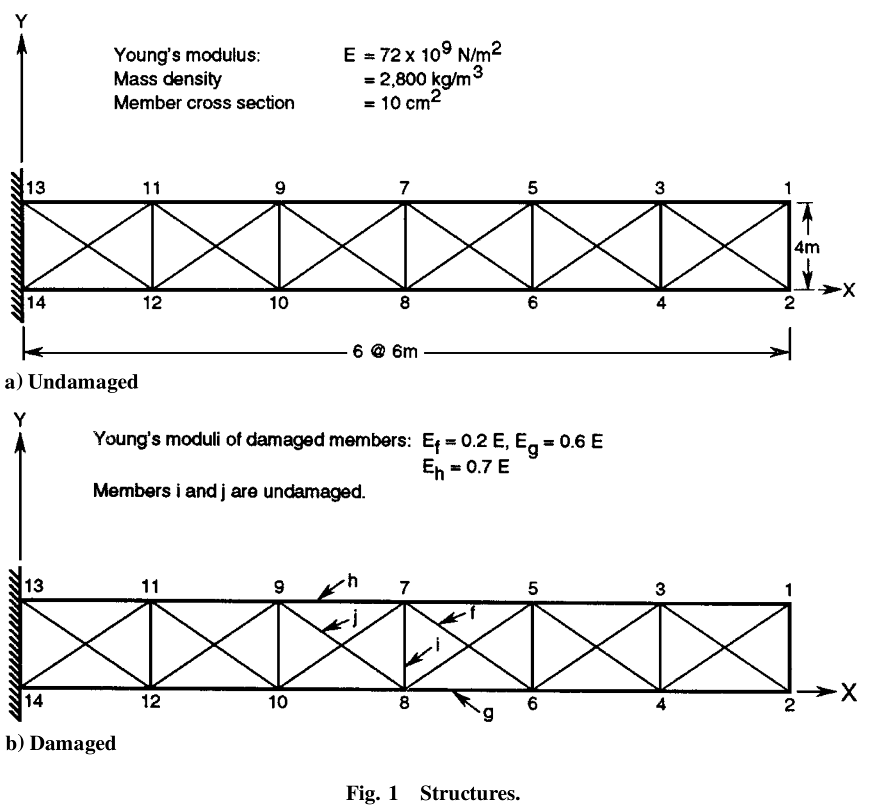

Fig. 1 Structures.

Table 2 Unity check errors for damaged structure

Node	Direction	Measured modes used: Four	Eight
1	*X*	0.00	0.03
	Y	0.01	0.00
2	*X*	0.01	0.02
	Y	0.01	0.00
3	*X*	0.01	0.02
	Y	0.01	0.03
4	*X*	0.02	0.05
	Y	0.01	0.04
5	*X*	0.01	0.03
	Y	0.03	0.08
6	*X*[a]	1.52	1.42
	Y[a]	0.76	0.93
7	*X*[a]	1.44	1.39
	Y[a]	0.75	0.93
8	*X*[a]	2.20	2.13
	Y	0.02	0.06
9	*X*[a]	2.08	2.10
	Y	0.03	0.03
10	*X*	0.01	0.03
	Y	0.03	0.04
11	*X*	0.01	0.02
	Y	0.03	0.02
12	*X*	0.01	0.03
	Y	0.03	0.01

[a]Indicates a significantly affected degree of freedom.

Table 3 Percent stiffness reductions for damaged structure

Member	Exact reduction	Measured modes used: Four	Eight
f	80	77.2	80.9
g	40	39.7	40.3
h	30	29.6	30.1
i	0	0.0	−0.9
j	0	1.2	−0.7

modes. Members requiring many modes to be sufficiently exercised, such as those near the free end, will probably require many measured modes to detect their damage.

The simulated measured modes used in the example are perfectly orthogonal and free of error, but real measured modes are neither. The experimental errors will introduce additional unity check errors. The effectiveness of the proposed method in real application, wherein actual test data are used, is still an open question. Furthermore, the proposed method requires that the analytical model of the original structure should have been verified by a mode survey test. How well the model should correlate with the test data, for the proposed method to work, has not yet been established.

Conclusions

Using a test-verified analytical model of the original undamaged structure and measured normal modes obtained after damage has occurred, the proposed unity check method appears to be able to locate the damaged structural members and to determine their stiffness reductions. The effectiveness of the method has been demonstrated with a numerically simulated and idealized example. Applicability of the method to real structures using actual test data is yet to be explored.

References

[1]Dobson, B. J., "Modification of Finite Element Models Using Experimental Modal Analysis," *Proceedings of the 2nd International Modal Analysis Conference*, Union College, Schenectady, NY, 1984, pp. 593–601.

[2]Sidhu, J., and Ewins, D. J., "Correlation of Finite Element and Modal Test Studies of a Practical Structure," *Proceedings of the 2nd International Modal Analysis Conference*, Union College, Schenectady, NY, 1984, pp. 756–762.

[3]Ojalvo, I. U., and Pilon, D., "Diagnostics for Geometrically Locating Structural Math Model Errors from Modal Test Data," AIAA Paper 88-2358, April 1988.

[4]Gordis, J. H., "An Exact Formulation for Structural Dynamic Model Error Localization," *Proceedings of the 11th International Modal Analysis Conference*, Union College, Schenectady, NY, 1993, pp. 159–167.

[5]Lin, C. S., "Location of Modeling Errors Using Modal Test Data," *AIAA Journal*, Vol. 28, No. 9, 1990, pp. 1650–1654.

R. B. Malla
Associate Editor

Solar Array Degradation by Dust Impacts During Cometary Encounters

Ralph D. Lorenz*
University of Arizona, Tucson, Arizona 85721-0092

Introduction

THE effect of hypervelocity impact on spacecraft materials and structures is a subject that has received extensive attention in the context of space debris in Earth orbit. Motivated by forthcoming missions to small bodies and recent results on hypervelocity impacts on solar panels returned to Earth from the Hubble Space Telescope, I consider the damage to spacecraft solar arrays during the spacecraft flybys of comet Halley in 1986 and show that the performance loss seems to be related to the fluence of the smallest impactors and is around three orders of magnitude higher than would be expected from crater-area considerations. The nonlinearity and the magnitude of the solar array degradation with dust fluence are consistent with open-circuit failures of solar cell strings, possibly by impacts on or near cell interconnects.

Spacecraft Results

It is well known that solar array performance degrades in space, such that arrays need to be sized for their end-of-life performance. For example, in low Earth orbit (LEO) silicon solar arrays degrade by up to 3.75% per year, of which 2.5% is attributed to radiation damage.[1] The rest of the damage is attributed to other mechanisms such as thermal cycling, uv degradation, and micrometeoroid and debris strikes. How much damage is due to the latter effects is difficult to determine. However, the handful of cometary encounters to date allows the determination of array damage due to dust impact: the large dust fluence causes significant, and therefore measurable, array performance loss, there are simultaneous dust flux measurements, and the short duration of the degradation event eliminates most alternative damage mechanisms.

The two Russian Vega spacecraft were the first spacecraft[2] at comet Halley in 1986, and each had large, unprotected planar solar arrays and an instrument pointing platform. Although they came no closer than 8000 km to the nucleus, they both suffered severe dust damage due to the large dust fluence and the high impact velocity (78 kms^{-1}). Vega 1 lost its high- and low-frequency plasma wave analyzer, and Vega 2 lost the low-frequency plasma wave analyzer and its three-axis magnetometer. Also, they lost about 50% of their solar array generation capacity (Fig. 1).

The Giotto spacecraft[3] made a very close encounter[4] (~600 km at 69 kms^{-1}) with Halley soon thereafter. It had a cylindrical solar array behind a Whipple bumper shield. A large impact near closest approach generated a nutation, which may have exposed the array to dust impacts thereafter. The array may have also suffered some

Received Nov. 6, 1997; revision received March 23, 1998; accepted for publication April 27, 1998.

*Research Associate, Lunar and Planetary Laboratory, Department of Planetary Sciences.